

Adding Aramid Fibers to Improve Tribological Characteristics of two Polymers

M. Botan^a, A.E. Musteata^b, T.F. Ionescu^b, C. Georgescu^b, L. Deleanu^b

^aINCAS - National Institute for Aerospace Research "Elie Carafoli", Bucharest, Romania,

^b"Dunarea de Jos" University, Faculty of Engineering, 111 Domneasca, Galati, 800201, Romania.

Keywords:

Dry sliding
Aramid fibers
PBT
PA
Wear

ABSTRACT

This paper presents the influence of the matrix on tribological properties of composites having 10% aramid fibers. Polyamide (Relamid) and PBT (Crastin) were used as matrix. The short aramid fibers (Teijin) were approximately 200...250 μm in length and 10 μm in diameter, with expended extremities due to manufacturing process. Tests were done on block-on-ring tribotester on a BRUKER-CETR[®].UTM 2 system. The test parameters were: sliding speed (0.25, 0.50 and 0.75 m/s), the load (5, 10, 15 and 30 N) and the sliding distance of 5,000 m. There were analyzed the dependence of friction coefficient, temperature on the contact edge and wear of the polymeric materials. SEM images help identify wear mechanisms and pointed out the different behavior of the two matrixes. Adding aramid fibers into a matrix of either PA or PBT makes the resulting blends have better tribological characteristics: the wear is much lower, the friction coefficient slightly increases, but remaining in an acceptable range for actual applications as compared with the neat polymers. PBT + 10% wt aramid fibers had the lowest wear versus a slightly higher coefficient of friction as compared to that of PBT, for the tested regimes.

Corresponding author:

Lorena Deleanu
"Dunarea de Jos" University,
Faculty of Engineering,
111 Domneasca, Galati, 800201,
Romania.
E-mail: lorena.deleanu@ugal.ro

© 2017 Published by Faculty of Engineering

1. INTRODUCTION

Global energy and resources crisis has been made plastics find their field of application in virtually all industries, from the food, automotive, aviation, medicine and hi-tech technologies, where the polymeric materials become non-replaceable.

Researchers have been focused on tribology of polymer composites and blends because friction couples with at least one element made of

polymeric materials could have better behavior as compared to "classical" pair of materials, here including metal-metal contacts [1-3]. Tribological characteristics of polymers are improved by adding reinforcements (short fibers [4], nano and micro particles [5], made of metallic or ceramic materials [6-8]), solid lubricants, flame retardants etc. The most used fibers in polymeric matrixes are: glass fibers, carbon fibers and, recently introduced, aramid fibers. Companies [2,9] offer on the market many composites with short fibers (carbon,

glass, aramid) as reinforcement, giving mechanical characteristics of materials, but tribological characteristics are still reported by research institutes and academic staff. For PBT, the mechanical characteristics are higher (Young modulus, tensile limit) adding 10 % short fibers (aramid, glass) [2,10] but comparison of tribological features are still rare. Reports on polymeric blends with aramid fibers of various lengths were done: 6 mm [11,12], 3 mm [13], 0.25 mm [14], 0.15...0.2 mm [15].

The aim of this study is to offer a comparison between two composites with the same quantity of short aramid fibers, PA6 and PBT, as concerning the tribological behavior.

2. TEST METHODOLOGY

The materials involved in this research study were produced at the Research Institute for Synthetic Fibers Savinesti, Romania, using a moulding equipment type MI TP 100/50.

Polyamide grade Relamid and PBT grade Crastin were used as matrix (Tables 1 and 2). The short aramid fibers, as supplied by Teijin, were approximately 200...250 µm in length and 10 µm in diameter, with expended extremities due to the manufacturing process (Fig. 1) [16].

Table 1. Properties of PBT - CRAFTIN 6130 NC010® [17,18].

Characteristic	Value
Maximum working temperature, [°C]	110...180
Tensile limit, [MPa]	65
Thermal conductivity, [W/m·K]	0.25
Thermal expansion coefficient, [K ⁻¹]	90·10 ⁻⁵
Young modulus, [MPa]	3300
Strain at yield, [%]	23
Melting temperature, [°C]	235.6

Table 2. Properties of polyamide Relamid® [19].

Characteristic	Value
Maximum working temperature, [°C]	90-110
Tensile limit, [MPa]	42
Thermal conductivity at melt, [W/m·K]	0.22
Thermal expansion coefficient, [K ⁻¹]	200
Young modulus, [MPa]	922
Strain at break, [%]	109
Melting temperature, [°C]	232

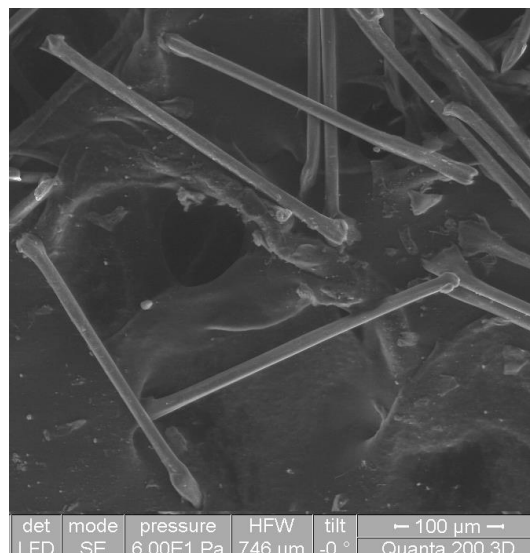


Fig. 1. Short aramid fibers, as supplied by Teijin.

The composites with either PA6 or PBT matrix and addition of aramid fibers and black carbon (Table 4) were produced on a micropilot plant, by die molding, with a single-screw extruder (length to diameter L/D = 25, D = 60 mm, Table 3), the cooling bath for the blank polymer, a granulator, a rotary dryer and rotary drum granules for mixing the constituent.

Table 3. Characteristics of the molding machine.

Characteristic	Value
Worm diameter, [mm]	33
Nominal power for pump, [kW]	11
Maximum molding volume, [cm ³]	96
Productivity, [kg/h]	40
Maximum molding pressure, [MPa]	114
Worm speed, [rpm]	20-250
Maximum stroke of the nozzle, [mm]	150
Maximum force on the nozzle, [kN]	35
Temperature range for material heating, [°C]	20-400
Maximum pressure of hydraulic oil, [MPa]	14

Table 4. Tested materials.

Symbol	Composition (%wt)
PA	100% PA
PAX	PA6 + 10% aramid fibers + 0.5% black carbon
PBT	100% PBT
PBX	PBT + 10% aramid fibers + 1% PA6 + 1% black carbon

The recommended parameters for polymer injection are [20]: temperature in feed zone - 220...240 °C, temperature of matrix - 70...90 °C, temperature in compression zone - 230...250 °C,

injection pressure - 80...120 MPa, temperature in mixing zone - 240...270 °C, the nozzle temperature - 250...260 °C.

Tests were done on block-on-ring tribotester (Fig. 2), included in a system BRUKER-CETR®.UTM 2 [21,22] with the parameters: sliding speed (0.25, 0.50 and 0.75 m/s), load (5, 10, 15 and 30 N) and the sliding distance of 5,000 m [23,24]. The speed of 0.5 m/s is the most used by producers of polymeric materials, for evaluating tribological properties [3].

There were analysed the dependence of friction coefficient, temperature on the contact edge with the help of a thermo-camera PI160 and dedicated soft PI Connect and wear (as mass loss of the block) on the material.

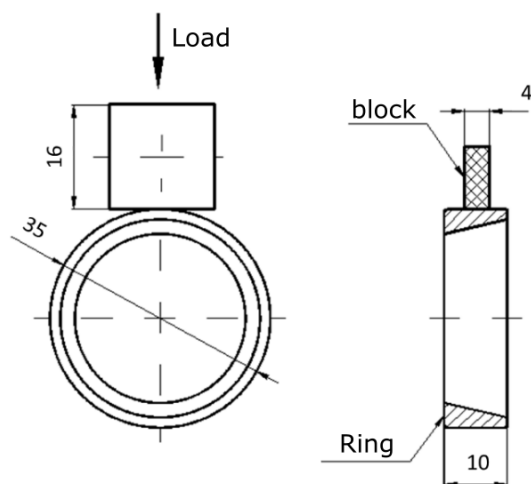


Fig. 2. Tribotester block-on-ring.

As one may notice from literature [23-25], the parameters for block-on-ring tests are in a wide range, especially for block dimensions, speed, load and sliding distance. After consulting many reports on this test, the authors considered that a sliding distance of 5000 m is satisfactory for making the friction coefficient and wear stable.

3. RESULTS

3.1 Friction coefficient

The average value of the friction coefficient (COF) was calculated for the running time of each test and the minimum and maximum values of this parameter are also given in Figs. 3 and 4. Comparing the average values for the neat polymer and the blend PAX, it is obvious that

load has a high influence after 15 N, the friction coefficient at 30 N being about three times greater for PA as compared to the blend.

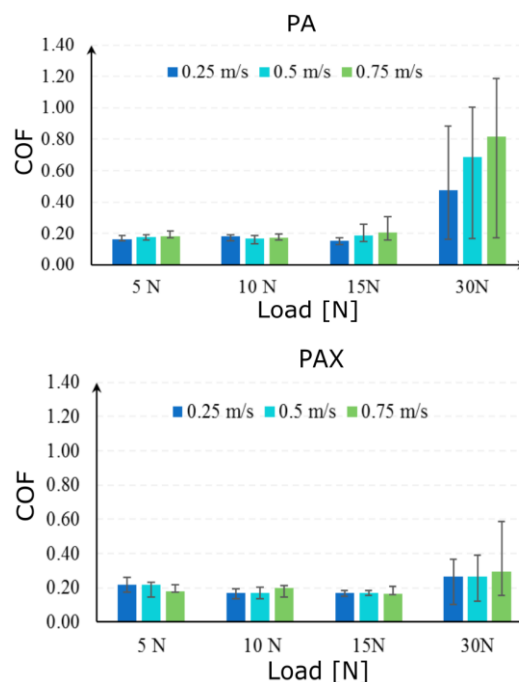


Fig. 3. Average and spread range for friction coefficient characterising the couple PA-steel and PAX-steel.

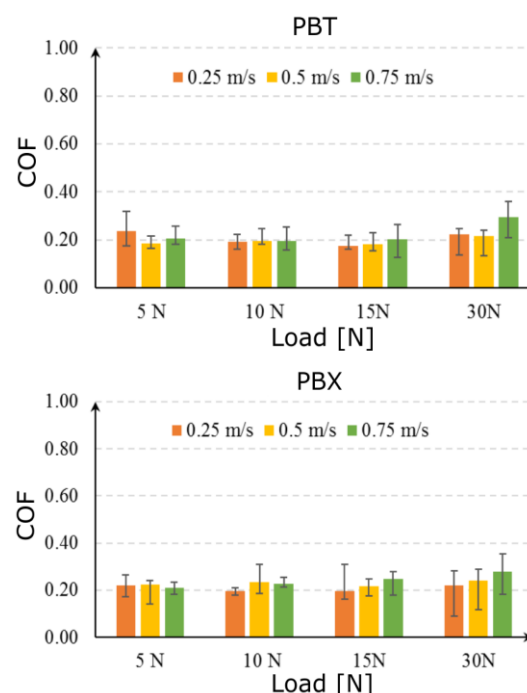


Fig. 4. Average and spread range for friction coefficient characterising the couple PBT-steel and PBX-steel.

For materials based on PBT, the differences in the average values of the friction coefficient are in a narrow range, thus, this tribological parameter is not relevant in selecting one of

these two materials and other tribological ones have to be compared (wear, running temperature, surface quality) [23,26].

In Figs. 3 and 4, the smallest average values of COF (around 0.2) were obtained for the test parameters $v = 0.25$ m/s, $F = 10$ N. The lower value of the spread range was obtained for $v = 0.25$ m/s and $F = 15$ N. In some systems, where smooth operation is required, it is good to know this range. Figures 5 and 6 show examples of the friction coefficient evolution in time for the analysed materials.

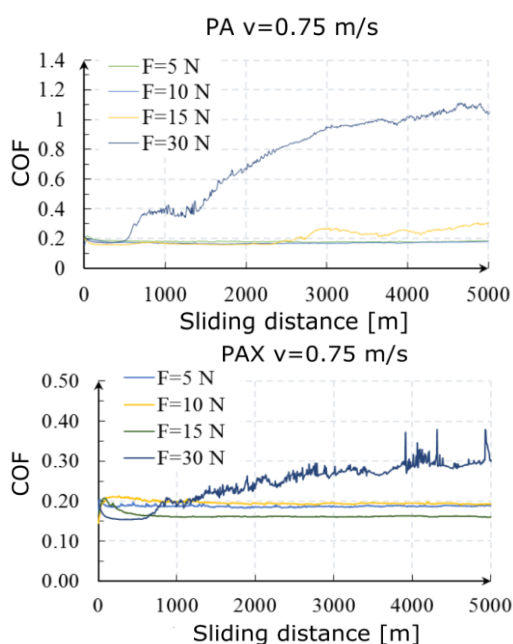


Fig. 5. Examples of COF evolution in time for PA and PAX.

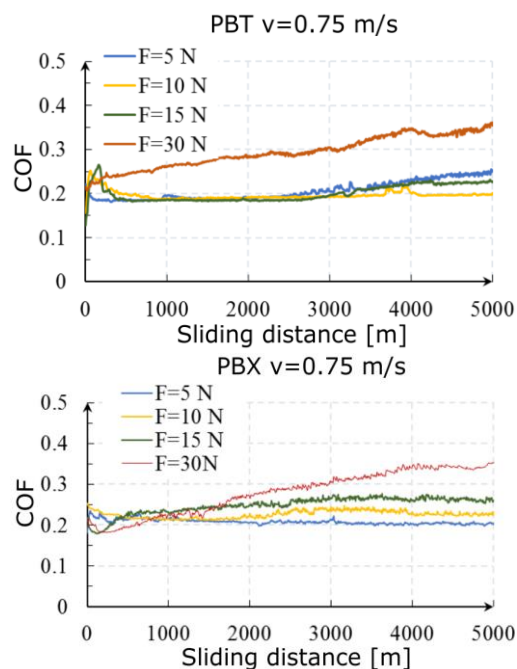


Fig. 6. Examples of COF evolution in time for PBT and PBX.

The following discussion is based Czichos's discussion on the friction coefficient [27] and Myshkin's studies [28].

For PA, one or two of these stages are missing and the friction coefficient has a smooth evolution in time for low loads, but for higher loads (15 N and 30 N), this parameter begins to increase after 2500...3000 m for $F = 15$ N and after a shorter sliding distance ($L = 600...1000$ m) for $F = 30$ N. This could be explained by the increasing temperature in contact (see Figs. 7-10) that favours the appearance of a soften/molten tribolayer that resists sliding more than the solid polymer. Adding 10% aramid fibers makes the friction coefficient becoming more stable for $F = 5...15$ N, but for $F = 30$ N, it increases and oscillates, not so severely as for the neat polymer.

For PBX, there could be identified several stages, but some are overlapping or they are missing, L being the sliding distance:

- phase I ($L = 0 - 200...500$ m) of adapting surfaces and an increasing friction coefficient, a step of adjusting the surface to increase the coefficient of friction, less pronounced at higher forces;
- phase II ($L = 200...500 - 1000$ m) a step in which the friction coefficient decreases because of the surface smoothing;
- phase III ($L = 1000 - 2500$ m) the friction coefficient is maintained at low values, possibly with a slight tendency to increase, more pronounced in composites;
- phase IV ($L = 2500...3000 - 5000$ m) - the development trend of the friction coefficient depends on the combination (load, speed, materials in contact).

3.2 Wear and temperature on contact edge

In this work, the authors defined wear mass as the mass loss of the block, the difference between the initial mass and the final element.

Wear maps have become a good tool for pointing out the influence of different parameters on wear [29]. Maps were plotted using a cubic interpolation in MATLAB R2009b and surfaces are "obliged" to include the experimental data. A point on a map represents a test for the same set of parameters (F [N], v [m/s], L [m]), where F is

the normal load, v is the sliding speed and L (5000 m) is the sliding distance. The values in temperature maps represent the temperature at contact edge, measured with a thermo-camera, just before the end of the test.

Figures 7 to 10 correlate the mass wear and the maximum temperature recorded on the edge of the contact. Looking at Fig. 7, for $F = 30$ N, materials based on PA6 have a sharp increase in the wear mass, very strong for $v = 0.75$ m/s. For example, at $v = 0.25$ m/s and $F = 30$ N, the wear of the PA block is 4.25 times higher than for a halved force ($F = 15$ N) and for $v = 0.5$ m/s, wear of PA block is 12 times higher than the wear at $F = 15$ N. The highest value was obtained at $F = 30$ N and $v = 0.75$ m/s. Based on these results, the authors recommend PA only in the field of $F = 5\text{--}15$ N and $v = 0.25\text{--}0.75$ m/s.

PAX had better results, but its wear for $F = 30$ N was noticeably higher (see Fig. 8) for $v = 0.50$ m/s and $v = 0.75$ m/s, but having similar values, which means a reduced susceptibility to wear speed variation. From $F = 15$ N to $F = 30$ N, PAX wear was increased by 1.5 times, at $v = 0.25$ m/s, increased 2.25 times for $v = 0.5$ m/s and wear was 10 times higher for $v = 0.75$ m/s.

PBX wear is greater than that of the PBT for $F = 5$ N (for all tested speeds) it follows that the addition is not justified for small loads. Starting from $F = 10$ N, the wear behavior of the two materials to a metal surface changes. Low values are obtained for the PBX. For $F = 30$ N, PBT wear is 2 times higher than that of the PBX, at $v = 0.25$ m/s and $v = 0.50$ m/s and 1.75 times for $v = 0.75$ m/s.

When comparing the values in Figs. 7 and 8, for the PA and PAX, to those in Figs. 9 and 10 for PBT and PBX, the following conclusions may be formulated.

For $F = 5$ N, PAX and PBX have higher mass wear, especially for low speeds as compared to the polymer PA and PBT, respectively. From $F = 10$ N to $F = 30$ N, additivated materials behaved better to wear, they have lost less material as compared to polymers without fibers.

Comparing wear values between PA and PBT, respectively PAX and PBX, favourable values (lower wear) are for PBT and PBX. PBT and PBX are less sensitive to changes in speed, regardless

of load, in other words, the authors recommend materials PBT and PBX, for processes where sliding speed changes substantially (in the range $v = 0.25\text{--}0.75$ m/s).

The maximum temperature recorded at the contact edge (Figs. 7-10) ranks the tribological behavior more clearly for the tested materials. A designer will be interested in a material which is not easily heated and the load and speed variations of load will induce or increase the temperature as low as possible.

PA had the largest increase in temperature in the same zone of test parameters (F, v), where the coefficient of friction and wear were maximum. PAX and PBT have similar peaks in the same zone, but minimum values of temperature are lower for PBT.

PAX has the minimum temperature in the range of $v = 0.25\text{--}0.50$ m/s and $F = 10\text{--}20$ N, while PBT has a larger area of combinations (F, v), for a temperature increase only a few degrees above the ambient temperature.

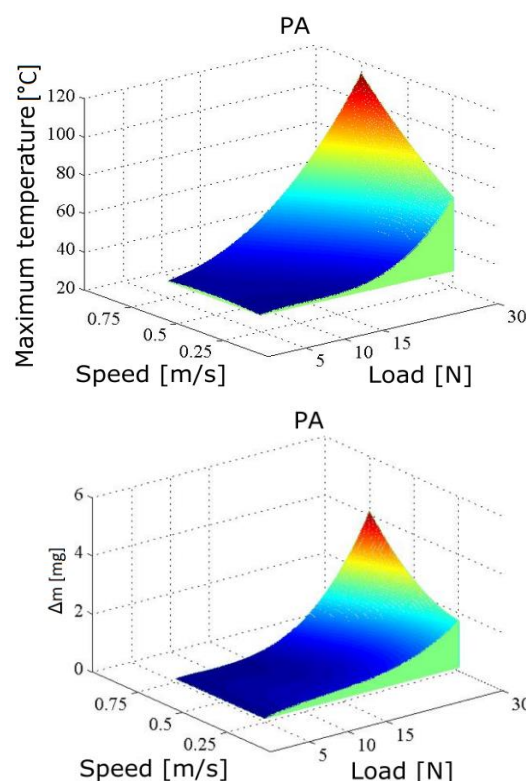


Fig. 7. Maximum temperature at contact edge and mass wear for PA.

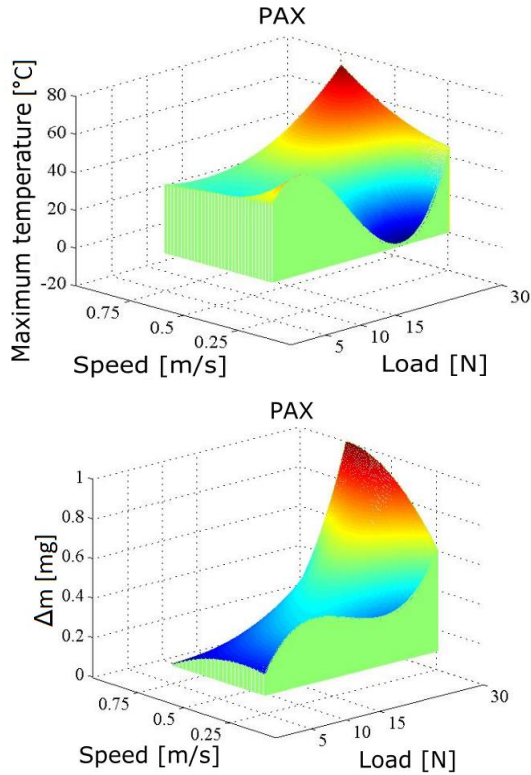


Fig. 8. Maximum temperature at contact edge and mass wear for PAX.

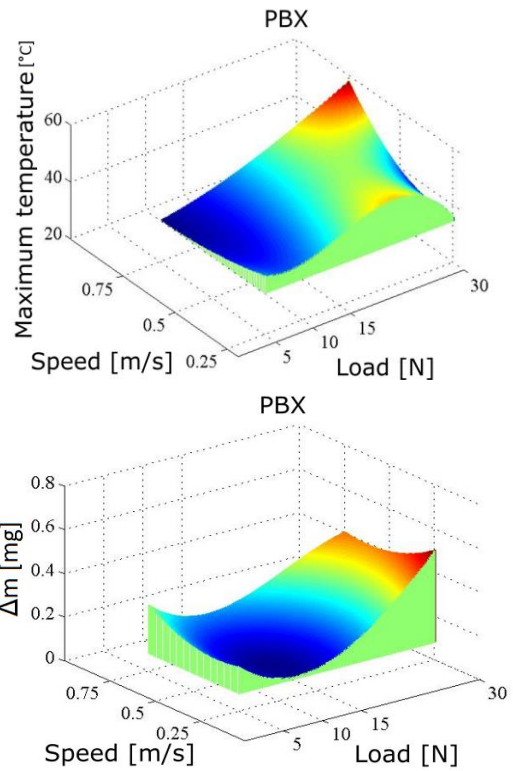


Fig. 10. Maximum temperature at contact edge and mass wear for PBX.

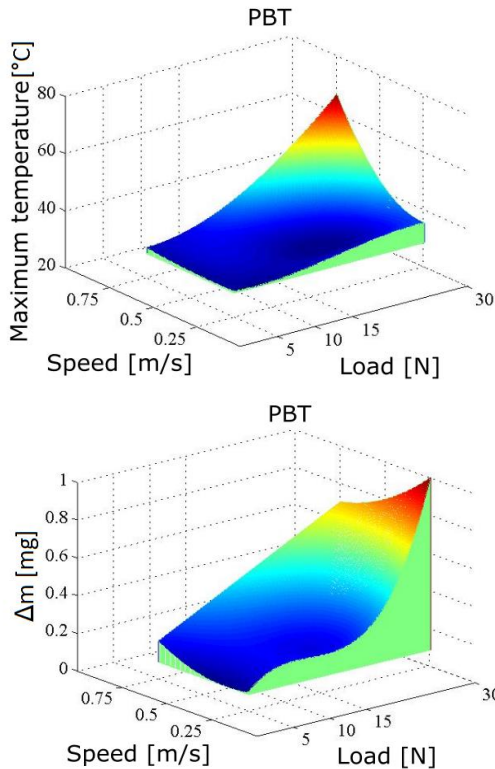
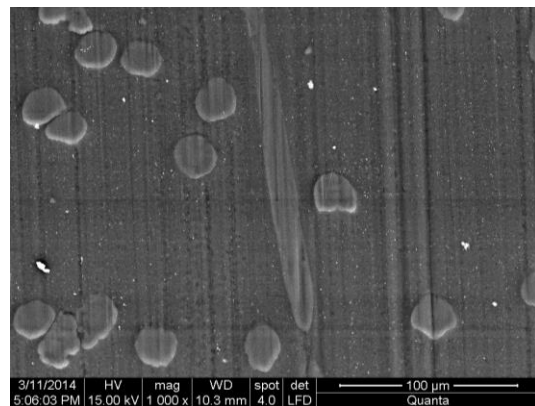


Fig. 9. Maximum temperature at contact edge and mass wear for PBT.

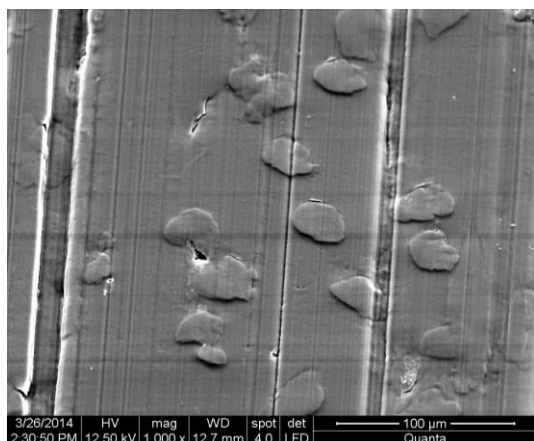
3.3 Wear mechanisms

PBX does not exceed 60 °C for any of the arrangements of test parameters.

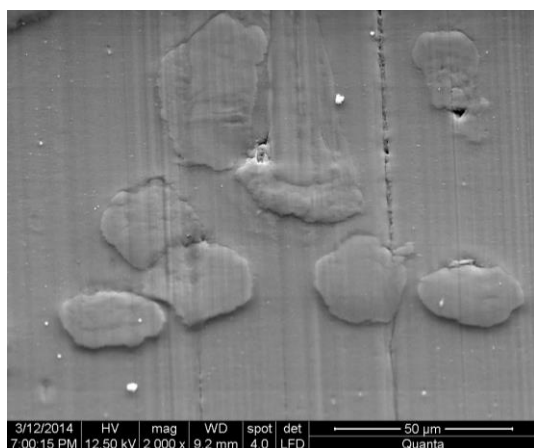
Friction couples involving at least one element made of polymeric materials initiate and develop particular wear mechanisms: transfer, particle agglomerations and compacting zones, abrasion (Fig. 11), all these influencing the tribological behavior.



a) PAX, $v = 0.25$ m/s, $F = 30$ N



b) $v=0.25$ m/s, $F=15$ N, PBX

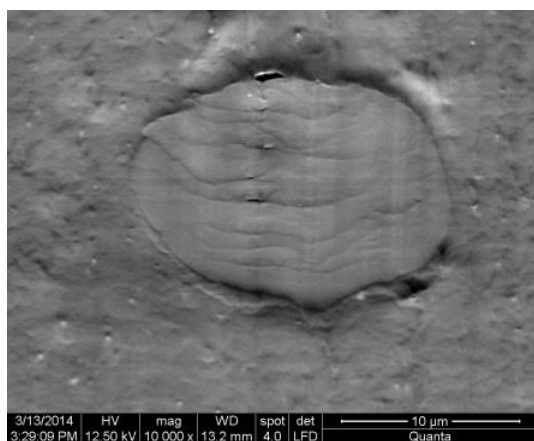


c) $v=0.75$ m/s, $F=30$ N, PBX

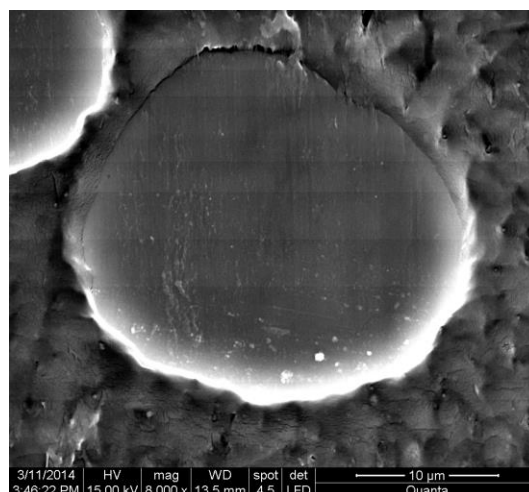
Fig. 11. Abrasion process on the polymeric block.

SEM images help identify wear mechanisms and pointed out the different behavior of the two matrixes.

Figures 12 and 13 shows a good bonding of the matrix around the fibers. Fibers are elastic and bend a little in the sliding direction, „opening” a small cavity between matrix and fiber, in front of the contact, as also described by Stachowiack [29].

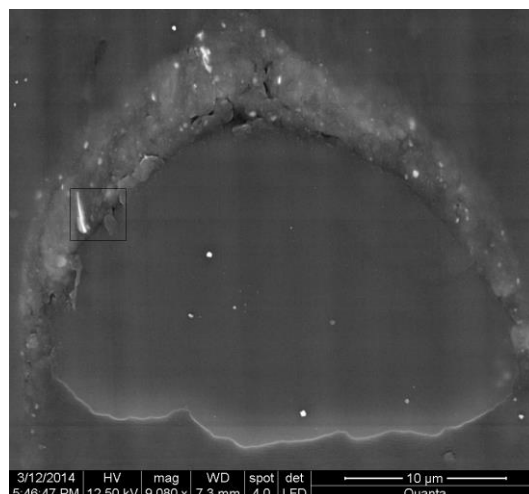


a) $v = 0.25$ m/s

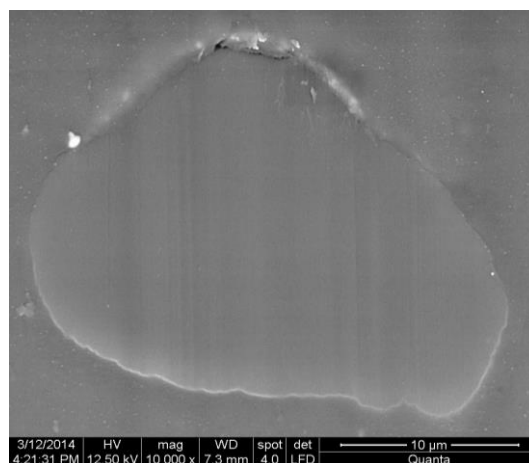


b) $v = 0.75$ m/s

Fig. 12. PAX, $F = 30$ N (sliding direction up-down).



a) $v = 0.5$ m/s



b) $v = 0.75$ m/s

Fig. 13. PBX, $F = 30$ N (sliding direction up-down).

Abrasion has ploughing as dominant process (Fig. 11a and 11b). This process is less intense for higher speed due to the softening of the tribolayer and the recovery of the polymeric

matrix. There is a debonding process between fibers and matrix, but the elasticity of aramid fibers diminishes the process intensity and the cavity so formed is easily fill with the smallest wear debris (Fig. 13). It seems that fibers are not broken when they are still embedded in the matrix, but after a running time, the polymer matrix is more prone to be detached and lets the fibers to be tear off, especially when they are approximately positioned parallel to the sliding direction (Fig. 11a and Fig. 14).

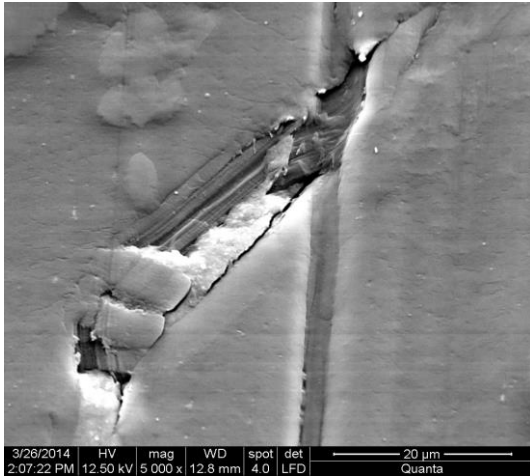
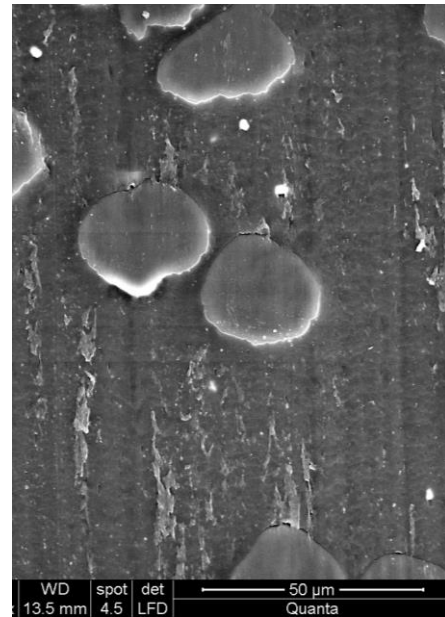


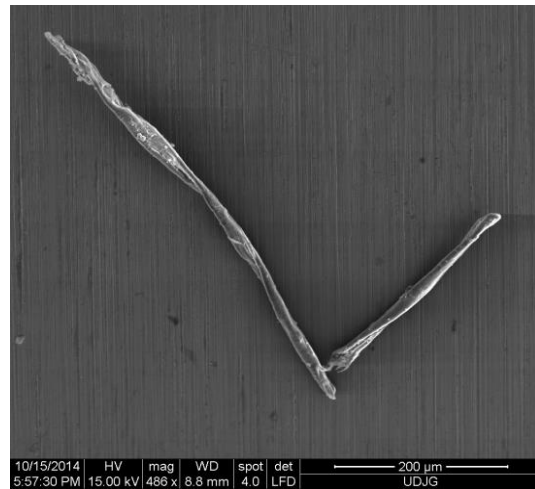
Fig. 14. Damage of the superficial layer of a block made of PBX, F = 15 N, v = 0.75 m/s.

Figure 15 shows that at v = 0.75 m/s, for the block made of PAX, the running regime makes a very thin layer of polyamide to be soften and molt. At v = 0.5 m/s this thin layer is not noticeable (Fig. 15a). Figure 16 presents a fiber detached from PAX, dragged and rolled in the contact (a), till break (b).

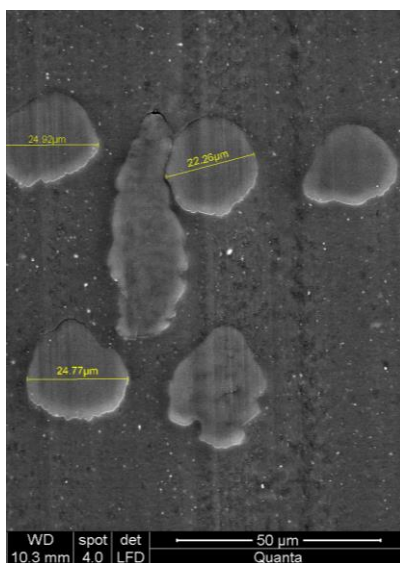


b) v = 0.75 m/s

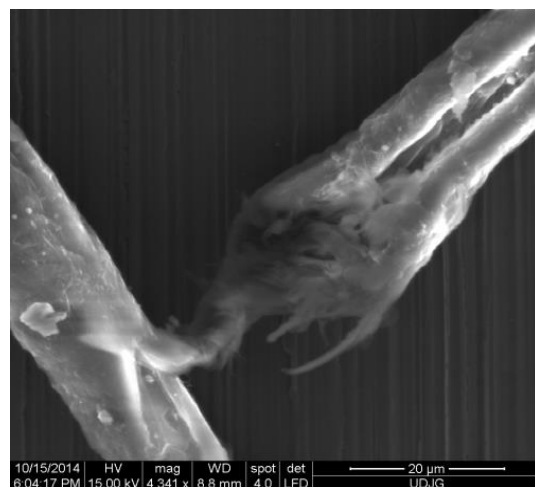
Fig. 15. Worn surface of a block made of PAX, F = 30 N.



a) Detached fiber



a) v = 0.5 m/s



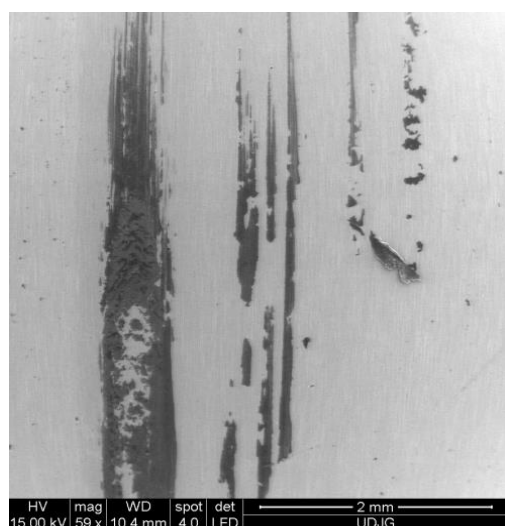
b) Detail

Fig. 16. Detached fiber, find on steel surface, PAX, F = 15 N, v = 0.25 m/s.

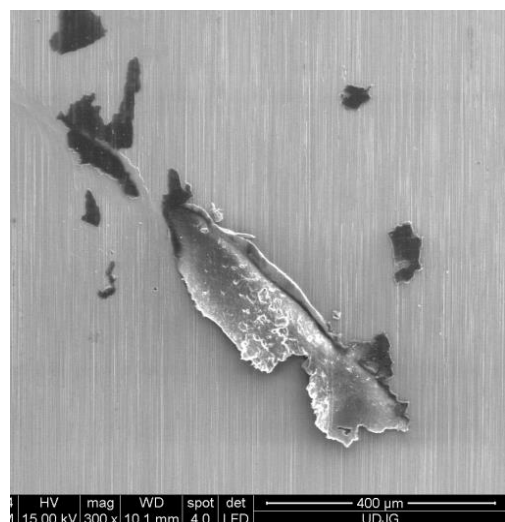
Relatively low melt temperature combined with the low thermal conductivity of polymers ensures that frictional heat generated in contact can easily reach the melting point of the polymer and cause its surface to melt, at least to soften.

When the polymer melts, its friction and wear parameter are markedly altered. The melt process is taking place in a very thin layer but now, it could be easier detached or spread on the surface. When this mechanism is prevailing, the type of material loss is named 'melting wear' [3]. Also, the transfer of polymer could be intensified.

Figures 17 and 18 present details of polymeric transfer on the steel surface of the ring and how the fibers are fragmented.

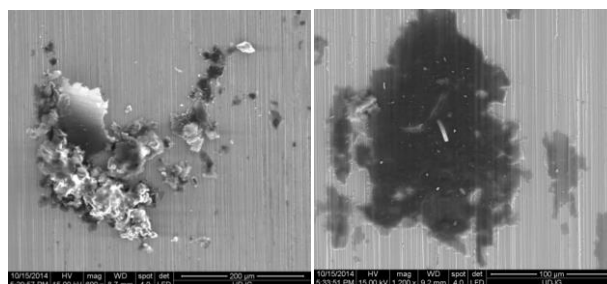


a) Lump transfer



b) Detail

Fig. 17. Steel ring surface after running against PBX ($F = 15 \text{ N}$, $v = 0,75 \text{ m/s}$).

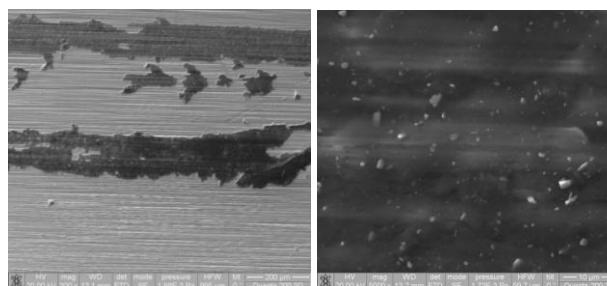


a) Adhesion and wear debris agglomeration

b) Lump transfer and trapped fragments of aramid fibers

Fig. 18. Steel ring surface after running against PAX, $F = 15 \text{ N}$, $v = 0.25 \text{ m/s}$.

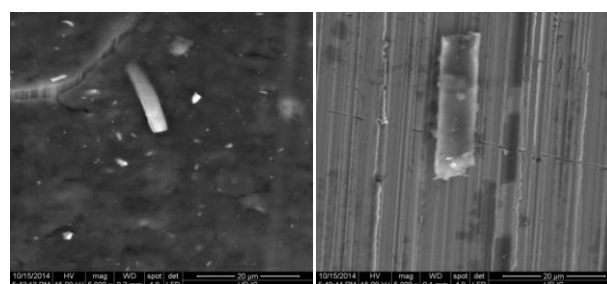
The separated fibers from the matrix do not break easily, but, in time, they are fragmented in small parts of several microns, as see in Fig. 19.b and Fig. 20.



a) Lump transfer

b) Detail

Fig. 19. PBX transfer on the steel ring ($F = 10 \text{ N}$, $v = 0.25 \text{ m/s}$).



a) Fragment of aramid fiber ambedded in an island transferred film

b) Fragment of aramid fiber, trapped in the steel surface asperities

Fig. 20. Fragments of aramid fibers on the metallic surface , block made of PAX, $F = 15 \text{ N}$, $v = 0.25 \text{ m/s}$.

4. CONCLUSIONS

From this tribological study, it results that adding 10 wt.% aramid fibers in PA and PBT decreases wear and the temperature in contact. The friction coefficient slightly increases for the materials containing aramid

fibers, but remaining in an acceptable range for actual applications.

The wear map of PA points out a zone with low wear for $F = 5 \dots 20$ N (1.25... 5 N/mm) and $v = 0.25 \dots 0.75$ m/s. For $F = 20 \dots 30$ N (5 ... 7.50 N/mm) and $v = 0.50 \dots 0.75$ m/s, the wear has a large gradient, indicating that the material should not be recommended for this regime.

Maps of wear recommend certain areas for load and speed in actual applications. Thus, it appears that PA and PAX wear is large for combination (high speed - high load), the polymer having a maximum of 4 times greater wear than PAX. PBT has an area of high wear for (high force - low speed) and the PBX had the lowest wear values, with a weak dependence on the sliding speed, especially for high load ($F = 30$ N).

The addition of 10 % aramid fibers in PA leads to flattening of the surface of wear map. The maximum value recorded for PAX is obtained for small forces and low speeds. So, this material has a much better wear behavior. PAX performs better at high speeds and for $F = 30$ N, curve shape of wear departs only slightly from a straight line.

For PBT, the resulting map shows a better behavior between 12 ... 24 N and velocity $v = 0.25 \dots 0.6$ m/s. The greatest wear was obtained for the combination (the lowest force - the highest speed).

It has been found that PBT without reinforcement has a very good tribological behavior, the average coefficient of friction being low and also a relatively low wear, but the addition of 10 wt.% aramid fibers, causes a substantial improvement in the wear behavior. PBT + 10 wt.% aramid fibers had the lowest wear versus a slightly higher coefficient of friction as compared to that of PBT, for the tested regimes.

Acknowledgment

This paper was presented at the 15th International Conference on Tribology, SERBIATRIB '17, Kragujevac, Serbia, 17–19 May 2017.

REFERENCES

- [1] K. Friedrich, Z. Zhang and A.K. Schlarb, 'Effects of various fillers on the sliding wear of polymer composites', *Composites Science and Technology*, vol. 65, no. 15-16, pp. 2329–2343, 2005.
- [2] Wear Resistant & Low Friction Thermoplastic Compounds, available at: <https://www.rtpcompany.com/products/wear-resistant/>, accessed: 22.04.2017.
- [3] B.J. Briscoe, S.K. Sinha, *Tribology of polymeric solids and their composites*, in G.W. Stachowiack (Ed.): *Wear – Materials, Mechanisms and Practice*, Wiley, New York, pp. 223–267, 2005.
- [4] D. Rus and L. Capitanu, 'Wear of Polished Steel Surfaces in Dry Friction Linear Contact on Polymer Composites with Glass Fibres', *Tribology in Industry*, vol. 35, no. 4, pp. 337-344, 2013.
- [5] I.O. Oladele, J.L. Olajide and M. Amujede, 'Wear Resistance and Mechanical Behaviour of Epoxy/Mollusk Shell Biocomposites developed for Structural Applications', *Tribology in Industry*, vol. 38, no. 3, pp. 347-360, 2016.
- [6] S.K. Sinha, B.J. Briscoe, *Polymer tribology*. London: Imperial College Press, 2009.
- [7] I.G. Bîrsan, A. Cîrciumaru, V. Bria and V. Ungureanu, 'Tribological and Electrical Properties of Filled Epoxy', *Tribology in Industry*, vol. 31, no. 1&2, 2009.
- [8] J. Quintelier, P. Samyn, P. de Baets, W. Ost and W. van Paepegem, 'Wear of Steel Against Carbon Fibre Reinforced PPS', *Tribology in Industry*, vol. 27, no. 3&4, 2005.
- [9] Low-Friction Mechanical Plastics, available at: <http://www.dupont.com/products-and-services/plastics-polymers-resins/articles/mechanical-plastic-low-friction.html>, accessed: 14.04.2017.
- [10] M. Botan, C. Georgescu, C. Pirvu and L. Deleanu, 'Influence of aramid fibers on mechanical properties of two polymeric blends', in *Proceedings of the 22nd International Conference on Materials and Technology*, Portoroz, Slovenia, 2014, p. 53.
- [11] M. Arroyo, R. Zitzumbo and F. Avalos, 'Composites based on PP/EPDM blends and aramid short fibres. Morphology/behaviour relationship', *Polymer*, vol. 41, no. 16, pp. 6351–6359, 2000.
- [12] M.A. López-Manchado, J. Biagiotti and J.M. Kenny, 'Comparative study of the effects of different fibers on the processing and properties of polypropylene matrix composites', *Journal of*

- Thermoplastic Composite Materials*, vol. 15, no. 4, pp. 337-353, 2002.
- [13] M. Shirazi and J.W. Noordermeer, 'Factors influencing reinforcement of NR and EPDM rubbers with short aramid fibers', *Rubber Chemistry and Technology*, vol. 84, no. 2, pp. 187-199, 2011.
- [14] G. Tang, W. Huang, D. Chang, W. Nie, W. Mi and W. Yan, 'The Friction and Wear of Aramid Fiber-Reinforced Polyamide 6 Composites Filled with Nano-MoS₂', *Polymer - Plastics Technology and Engineering*, vol. 50, no. 15, pp. 1537-1540, 2011.
- [15] M. Sanchez-Soto, A. Gordillo, M.L.L. Maspocho, J.I. Velasco, O.O. Santana and A.B. Martinez, 'Glass bead filled polystyrene composites: morphology and fracture', *Polymer bulletin*, vol. 47, no. 6, pp. 587-594, 2002.
- [16] Teijin Aramid Properties of Twaron, available at: <http://www.teijinaramid.com/aramids/twaron/>, accessed: 10.04.2017.
- [17] DuPont Engineering Polymers. Blow Moulding Processing Manual, available at: http://www2.dupont.com/Plastics/en_US/assets/downloads/processing/BM_PM_e.pdf, accessed: 10.04.2017.
- [18] DuPont. Crastin® PBT. Thermoplastic polyester resin Crastin® 6130 NC010, available at: <http://plastics.dupont.com/plastics/dsheets/crastin/CRASTIN6130NC010.pdf>, accessed: 10.04.2017.
- [19] M. Botan, 'Caracterizarea mecanică și tribologică a unei clase de compozite polimerice', *PhD thesis*, „Dunarea de Jos“ University, Galati, 2014.
- [20] Crastin PBT. Molding Guide, available at: http://www2.dupont.com/Plastics/en_US/assets/downloads/processing/cramge.pdf, accessed: 14.04.2017.
- [21] CETR UMT Multi-Specimen Test System, Software Operating Manual, Version 1.116, Build 222, 2007.
- [22] CETR UMT Multi-Specimen Test System, Hardware Manual, 2007.
- [23] C. Georgescu, 'Studii și cercetări privind evoluția parametrilor stratului superficial în procesele de frecare și uzură ale unor materiale compozite cu matrice de polibutilentereftalat', *PhD thesis*, „Dunarea de Jos“ University, Galati, 2012.
- [24] Z. Rasheva, G. Zhang and T.A. Burkhart, 'Correlation between the tribological and mechanical properties of short carbon fibers reinforced PEEK materials with different fiber orientations', *Tribology International*, vol. 43, no. 8, pp. 1430-1437, 2010.
- [25] G. Zhang, Z. Rasheva and A.K. Schlarb, 'Friction and wear variations of short carbon fiber (SCF)/PTFE/graphite (10vol.%) filled PEEK: Effects of fiber orientation and nominal contact pressure', *Wear*, vol. 268, no. 7, pp. 893-899, 2010.
- [26] L. Maftai, 'Contribuții la studiul comportării tribologice a compozitelor cu poliamidă și microsferă de sticlă', *PhD thesis*, „Dunarea de Jos“ University, Galati, 2010.
- [27] H. Czichos, *Tribology: a systems approach to the science and technology of friction, lubrication, and wear*. Amsterdam: Elsevier, 1978.
- [28] N.K. Myshkin, M.I. Petrokovets and A.V. Kovalev, 'Tribology of polymers: adhesion, friction, wear, and mass-transfer', *Tribology International*, vol. 38, no. 11, pp. 910-921, 2006.
- [29] S.M. Hsu, M.C. Shen, *Wear Mapping of Materials*, in G.W. Stachowiak (Ed.): *Wear - Materials, Mechanisms and Practice*, Wiley, New York, pp. 369-424, 2005.